Effect of hexafluoroisopropanol alcohol on the structure of melittin: A molecular dynamics simulation study

DANILO ROCCATANO,[1] MARCO FIORONI,[2] MARTIN ZACHARIAS,[1] AND GIORGIO COLOMBO[3]

[1]School of Engineering and Science, International University of Bremen, D-28725 Bremen, Germany
[2]Department of Chemistry, University of Indiana, Bloomington, Indiana 47405, USA
[3]Istituto di Chimica del Riconoscimento Molecolare, CNR, 20131 Milano, Italy

(RECEIVED March 9, 2005; FINAL REVISION June 14, 2005; ACCEPTED July 6, 2005)

Abstract

The molecular mechanism by which HFIP stabilizes the α-helical structure of peptides is not well understood. In the present study, we use melittin as a model to gain insight into the details of the atomistic interactions of HFIP with the peptide. We have performed extensive comparative molecular dynamics simulations (up to 100 nsec) in the absence and in the presence of HFIP. In agreement with recent NMR experiments, the simulations show rapid loss of tertiary structure in water at pH 2 but much higher helicity in 35% HFIP. The MD simulations also indicate that melittin adopts a highly dynamic global structure in 35% HFIP solution with two α-helical segments sampling a wide range of angular orientations. The analysis of the HFIP distribution shows the tendency of HFIP to aggregate around the peptide, increasing the local cosolvent concentration to more than two times that in the bulk concentration. The correlation of local peptide structure with HFIP coating suggests that displacement of water at the peptide surface is the main contribution of HFIP in stabilizing the secondary structure of melittin. Finally, a stabilizing effect promoted by the presence of counter-ions was also observed in the simulations.

Keywords: preferential solvation; peptide folding; α-helix stability; fluorinated alcohol; cosolvent effect; helix bending

1,1,1,3,3,3-Hexafluoro-propan-2-ol (HFIP) is one of the most effective cosolvents for the structural stabilization of secondary structure forming peptides. In particular, it is one of the strongest helix-inducing and stabilizing cosolvents (Hirota et al. 1997). The mechanism of peptide stabilization by fluorinated solvents has been investigated by experimental techniques (Buck 1998) and, more recently, by molecular dynamics simulations (Diaz et al. 2002; Fioroni et al. 2002; Roccatano et al. 2002). The results of these studies have evidenced the presence of a complex mechanism involving a combination of different contributions. In the case of 2,2,2-trifluoroethanol (TFE), computer simulations indicate a coating effect of the cosolvent on the simulated peptides, as a possible mechanism of peptide stabilization (Diaz et al. 2002; Fioroni et al. 2002; Roccatano et al. 2002). The coating effect is favored by the tendency of the fluorinated solvents to form large clusters in aqueous solution (Hong et al. 1999; Gast et al. 2001). The layer of cosolvent around the peptide reduces the accessibility of the backbone hydrogen bonds to the aqueous solvent, improving secondary structure stability.

Among the peptides used to study the effect of fluorinated solvents experimentally, melittin (MLT) is one of the most frequently investigated peptides. Melittin is a 26-

Reprint requests to: Danilo Roccatano, School of Engineering and Science, International University of Bremen, Campus Ring 1, D-28725 Bremen, Germany; e-mail: d.roccatano@iu-bremen.de; fax: +49-421-200-3249.

Article published online ahead of print. Article and publication date are at http://www.proteinscience.org/cgi/doi/10.1110/ps.051426605.

residue amphiphilic peptide with sequence GIGA VLKVLTTGLPALISWIKRKRQQ that constitutes one of the principal venom components from the honey bee *Apis mellifera*. Its toxic effect consists in the lysis of red cells in the blood of the punctured human. In water at low pH and low (< 0.01 M) ion concentration, MLT is monomeric and behaves as a random coil (Kempe et al. 1997). At higher pH, or at higher salt concentration, melittin starts to form monomeric α-helices that eventually aggregate to form tetramers. The α-helical conformation is induced by the presence of lipid micelles or bilayers, and in this conformation the peptide forms pores in the membrane. Similarly, the addition of cosolvents like HFIP or TFE also induces the formation of α-helical structures (Jasanoff and Fersht 1994; Hirota et al. 1997; Kempe et al. 1997; Hong et al. 1999).

The effect of alcoholic solvents or cosolvents on the stability of the melittin α-helix has been investigated previously by different authors using molecular simulation methods (Sessions et al. 1998; Fioroni et al. 2001; Roccatano et al. 2002; Liu and Hsu 2003). In simulation studies in methanol (Sessions et al. 1998) and in a membrane environment (Bernèche et al. 1998; Bachar and Becker 2000), melittin stayed close to the experimental α-helical structure, whereas in water it starts to bend and unfolds (Roccatano et al. 2002). Short MD simulations (5 nsec) of melittin in 30% (v/v) HFIP/water mixture have already been performed to test the HFIP parameterization (Fioroni et al. 2001). However, this study did not include a systematic analysis of the conformational preference of melittin in HFIP and the molecular mechanism of how HFIP stabilizes the structure of melittin. In a recent article, Gerig (2004) reported an extensive NMR spectroscopic study on the structure of melittin in 35% HFIP/water mixture. The result of this study indicates the presence of a bent structure with two fluctuating α-helices.

In the present study, we perform extensive simulations (100 nsec) of melittin in water and in 35% HFIP/water mixture in order to investigate at the molecular level the structural and dynamic effects of HFIP on this peptide. Furthermore, we also analyzed the effect of counter-ions on the stability of the α-helix. The effect of counter-ions on protein stability has been investigated by different authors (Ibragimova and Wade 1998; Sessions et al. 1998; Pfeiffer et al. 1999; Walser et al. 2001). In the case of melittin, an earlier MD simulation in methanol has shown that the presence of counter-ions can produce sensitive effects on structural stability within a few hundred picoseconds (Sessions et al. 1998). The present comparative simulation studies starting from the X-ray structure indicate that melittin rapidly unfolds in water under low pH conditions in agreement with experiment. In 35% HFIP, the helical structure is largely preserved with an average global conformation in good agreement with NMR data. However, the partial unfolding of the helices is seen toward the end of the simulation. Addition of salt slows down the unfolding process both in 35% HFIP and in water. The analysis of the distribution of HFIP molecules around the peptide allows drawing conclusions on the mechanism of structure stabilization by HFIP and the mechanism of helix bending and unfolding.

Results

In Figure 1, the secondary structure analysis of melittin is reported for all the simulations. In the absence of

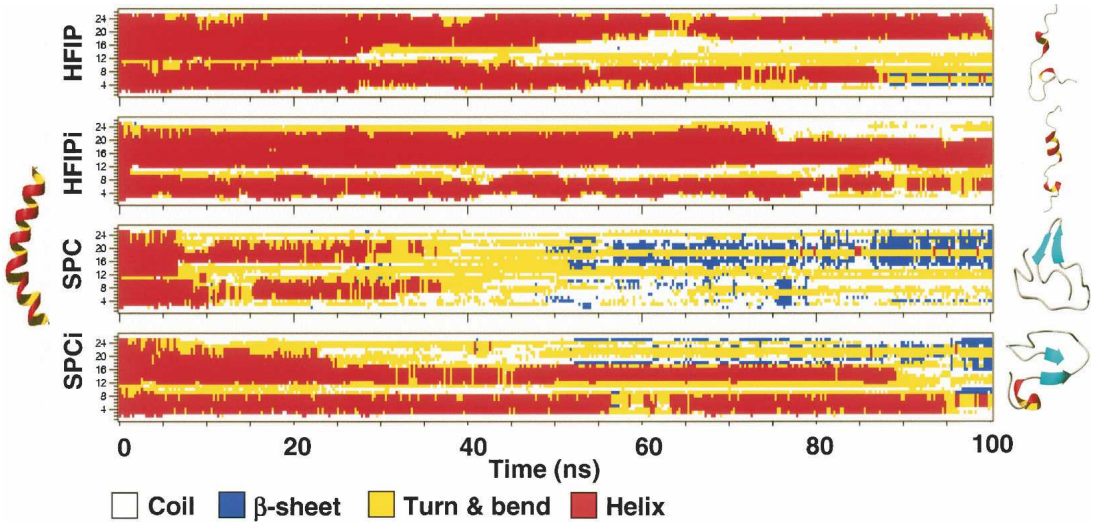

Figure 1. Time course of the secondary structure for the two simulations. The secondary structure definitions are based on the Kabsch-Sander DSSP definition (Kabsch and Sander 1983).

HFIP, the conservation of the helical structure in the course of the simulations depends substantially on the presence or the absence of the counter-ions. The SPC simulation completely loses the helical secondary structure of melittin after 20 nsec, while in SPCi, it remains stable for almost 70 nsec. Interestingly, the C-terminal region is less stable, and at the end of the simulation, it tends to form a β-hairpin structure. In the case of HFIP/water simulations, the peptide shows more defined helical segments during the simulations in the presence and absence of ions. However, in the HFIPi simulation, the α-helical regions are longer. The central region of the peptide (residues 9–11) loses its initial helical structure. Interestingly, the structure shows folding/unfolding events of α-helical fragments.

In Figure 2, the time average of the α-helicity is reported for all the simulations. If we consider as threshold an α-helicity value of 20%, the boundaries of the first helix are comprised between 3 and 7 for the SPCi and HFIPi simulations, and 3 and 8 for the HFIP simulation. The experimental NMR data indicate the range 2–8 (Gerig 2004). The second helix starts at residue 12 for the SPCi and HFIPi simulations. In the SPCi simulation, the helix ends after residue 16, while in the HFIPi simulation, the original helicity is maintained until residue 21. In the case of HFIP, the helical structure extends up to residue 24.

In Figure 3, the time course of the angle (α) between the axes of the two α-helices (see Fig. 3) in all the simulations is reported. In all the simulations, the initial angle $\alpha = 129^{\circ}$ (as in the X-ray structure) is generally lost within 10 nsec. With the exception of the SPCi simulation, subsequent oscillatory motions allow the angle to fluctuate and recover the initial value for a few nanoseconds. In the case of SPC water simulations (Fig. 3, bottom panel), the angle recording was extended until

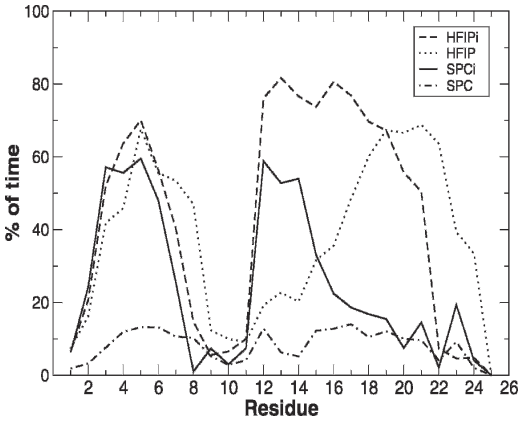

Figure 2. Time average of α-helicity per residue of MLT in the four simulations.

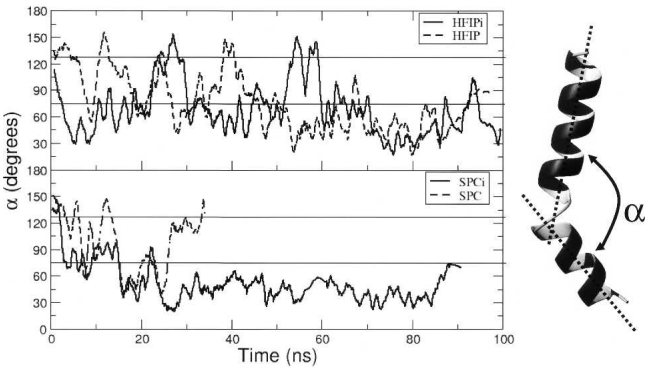

Figure 3. Time course of the angle α between the two helix segments present during the simulations.

the disruption of one or both helical segments. In the case of the SPCi simulation, the structure bends rapidly and then remains bent with an interhelix angle of $45^{\circ} \pm 3^{\circ}$ until the unfolding of both the helical segments at 90 nsec simulation time. The total average values along the course of the HFIPi simulation is $\alpha = 77^{\circ} \pm 11^{\circ}$, in close agreement with the value obtained from NMR experiments of $\alpha = 73^{\circ} \pm 15^{\circ}$ (Gerig 2004). In the case of HFIP simulation, the conformations stabilize after 40 nsec around an average value of $\alpha = 59^{\circ} \pm 9^{\circ}$, until the time of 85 nsec, where the N-terminal helix loses its structure.

To characterize the conformational variability in the sampled structures, a clustering analysis was performed on all four simulations. In Figure 4, the cumulative number of clusters for each simulation has been plotted as a function of time. From the analysis presented in Figure 4, it is evident that the number of clusters varies between the different simulations. In the case of solvent mixture simulations, the number of clusters is half of that present in water simulations. The larger number of clusters in the water simulations indicates the presence of an enhanced flexibility compared with the simulations in the presence of a 35% HFIP mixture. In the case of the HFIPi simulation, 14 clusters were obtained with the three largest ones representing 48%, 15%, and 14% of the trajectory, respectively. In the case of the HFIP simulation, the first three largest clusters represent 31%, 31%, and 10% of the trajectory, respectively.

In Figure 5, the representative structures obtained from the cluster analysis from both the simulations are reported. In the case of HFIP, the first cluster shows a structure very similar to the crystal structure, indicating a tendency of the peptide to stay in more extended conformations, as also indicated by the helix angle curve of Figure 3. On the contrary, the first two representative structures from the HFIPi simulation are bent, indicating a more pronounced tendency of the peptide to populate this state with respect to the HFIP case. A similar effect is evident in the pure

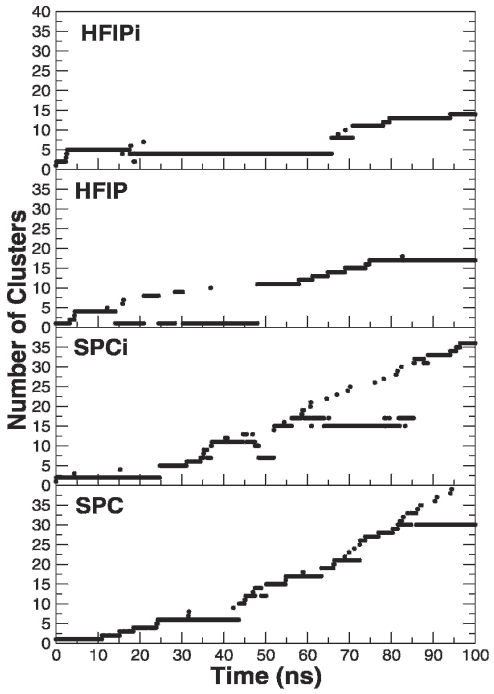

Figure 4. Time course of the different clusters of structures obtained for the different simulations.

water solvent simulations (see Fig. 3). A possible explanation for this difference can be related to the presence of counter-ions. The analysis of counter-ion distributions in the last 30 nsec of both SCPi and HFIPi simulations, shows that the Cl^- ions interact mainly with the charged side chains of the peptides, localized at the two ends. These interactions allow the charged ends to get closer since the repulsive positive charges are partially screened by the presence of the counter-ions.

In Table 1, the number of violations per residue from the experimental NOEs (Gerig 2004) are reported for the HFIPi and HFIP simulations. For both simulations, the violations are mainly observed in the weak (> 0.5 nm) and medium-weak NOE range (0.35–0.5 nm). The NOE deviations are mainly localized in the region with larger secondary structure variations, namely, at the C-terminal end and in proximity of the α-helix kink region. The total average value of these violations is 0.17 nm. The HFIP simulation shows a comparable number of violations in the same range. In this case, the total average value of the violations is 0.12 nm.

Preferential solvation

In Figure 6, the average LHC (local HFIP concentration) for each melittin residue versus the C_α–C^c_{HFIP} distance (where C^c_{HFIP} is the central HFIP carbon atom) calculated over the last 15 nsec of the HFIPi and HFIP simulations has been reported. The LHC within 0.6 nm (see Fig. 7) calculated over the full trajectory has an average value of 77% and 73% (v/v) for the HFIPi and HFIP simulations, respectively—namely, two times higher than the bulk. This indicates a strong tendency of the HFIP molecules to coat the helix. From the error bars of Figure 7, it appears that the LHC has small variations along both the trajectories. As expected, the largest fluctuations are in correspondence of regions where the peptide is more flexible. Figure 8 shows two snapshots of the last conformation from the HFIPi and HFIP simulations, respectively. In the figure, the solvent molecules within 0.6 nm from the melittin are represented, indicating the tendency of HFIP molecules to cluster around the peptide forming a coat that reduces the water concentration.

A correlation between the presence of α-helical structure and the increase of LHC around the peptide is present in both simulations. The residues belonging to the second helix segment show the largest concentration (Fig. 7). It appears that HFIP amplifies the local tendency of the peptide to form a preferred secondary structure. Regions with a high tendency to form an α-helix show enhanced coating that, in turn, stabilizes the helix. On the contrary, segments with higher flexibility (end regions and kink region) show a reduced coating (see Figs. 6, 7). It is worth noting that in the primary sequence these regions are rich in hydrophobic residues. These results suggest that HFIP displaces water from the immediate environment of the peptide, with a mechanism reminiscent of the hydrophobic effect. This, in turn, would decrease the chance of forming favorable interactions (such as hydrogen bonds) between either the backbone of the peptide and water or the amino acid side chains and water. These results are in line with the effect observed by simulation of the same peptide in TFE (Roccatano et al 2002).

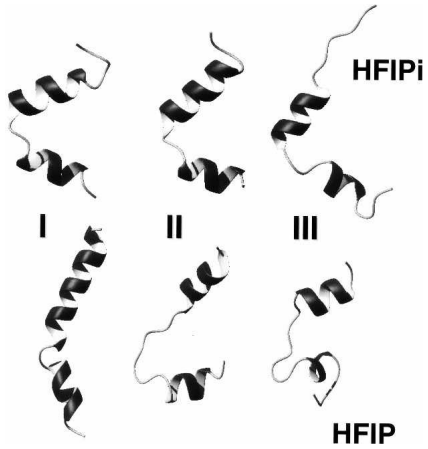

Figure 5. Representative structures of the three most populated clusters from the HFIPi and HFIP simulations, respectively.

Table 1. *Summary of the violations of the intramolecular ^1H $\{^1H\}$ NOE distance for the HFIPi and HFIP simulations*

Res. number	Residue name	Exp. data	HFIPi	HFIP
1	Gly	1	0	0
2	Ile	12	1	1
3	Gly	15	0	1
4	Ala	7	1	1
5	Val	14	1	0
6	Leu	14	1	1
7	Lys	14	2	1
8	Val	17	3	1
9	Leu	18	1	0
10	Thr	16	4	1
11	Thr	15	6	2
12	Gly	6	1	0
13	Leu	15	5	2
14	Pro	8	0	0
15	Ala	13	1	1
16	Leu	25	1	1
17	Ile	22	0	0
18	Ser	13	0	1
19	Trp	31	0	0
20	Ile	24	1	1
21	Lys	10	0	0
22	Arg	20	3	0
23	Lys	16	1	0
24	Arg	12	3	1
25	Gln	8	2	0
26	Gln	8	2	0
Total NOEs		229	20	8
Total s		1	0	0
Total m		74	2	1
Total m-w		76	13	6
Total w		78	5	1

In the third column, the total number of experimental NOEs per residue (intraresidue NOE are counted one time) are reported. In the last two columns, the number of violations for the HFIPi and HFIP simulations, calculated using the $\langle r^{-6}\rangle^{-1/6}$ averaging method, are reported, respectively. The NOEs are classified according to the upper distance restraints as follows: strong (s) = 0.25 nm, medium (m) = 0.35 nm, weak-medium (w-m) = 0.5 nm, weak (w) = 0.55 nm.

Discussion

A number of studies have shown that melittin conformation depends significantly on the solvent environment. In the crystal it adopts a helical structure; in a membrane, a partially helical conformation; and in water, it unfolds. Addition of fluorinated cosolvents can induce the helical structure. Melittin is an excellent model system to systematically study the effect of fluorinated cosolvents on the structure of peptides. The purpose of this study is to analyze the effect of HFIP on the melittin model system using comparative MD simulations on a timescale that goes much beyond any previous simulation on similar systems. At this level of simulation, our 100-nsec MD runs are not long enough to sample with the proper statistical weight folding and unfolding events. Longer simulations or multiple replicas of the trajectories should, in fact, be used to define the broad distribution of conformational first passage times. However, they can give qualitative insight on the interactions of added fluorinated (membrane-mimicking) cosolvents with helical peptides.

The comparative MD simulations indicate that the NOE distance-bound violations, summarized in Table 1, show that both the simulations in 35% HFIPi and HFIP explore regions of conformational space in which the peptide fulfills most of the available NMR-derived constraints. The overall agreement with experimental data is qualitatively good. The observed violations are among the weak-medium NOEs with very few in the medium range. One explanation for the violations could be that in solution, only a fraction of the peptide conformations contribute to some of the experimentally observed NOEs. However, these violations can also be considered as the result of an incomplete sampling of the conformational space accessible to the peptide (Colombo et al. 2002, 2003), and more extended simulations are required to obtain more accurate data. Furthermore, in the case of the HFIP simulation, it is interesting to note that although there is an evident loss of secondary structure detected by the DSSP analysis (Fig. 1), the NOE constraints are still mostly satisfied. The weak correspondence of the secondary structure with the overall folding of the structure was already observed in the simulation of other peptides (Colombo et al. 2002). In the simulations it was also observed that HFIP molecules surrounding the peptides limit the accessibility of water to the surface. A similar behavior was observed for simulations of peptides in TFE/water mixtures (Roccatano et al. 2002). In the case of TFE, this effect was supported by the results of NMR diffusion measurements and MD calculations on other peptides (Diaz et al. 2002; Fioroni et al. 2002). The results of the

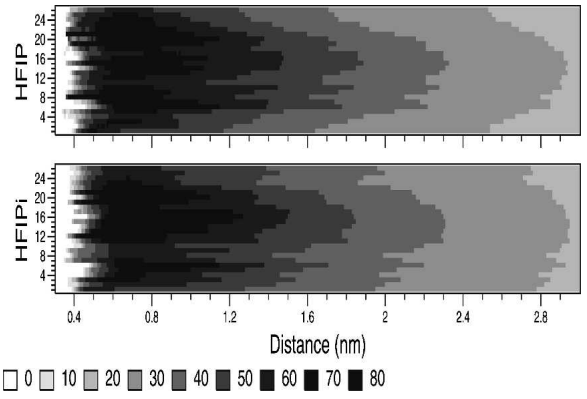

Figure 6. Local HFIP concentration vs. the distance from the C_α atom of each residue of melittin, calculated for the last 15 nsec of both simulations.

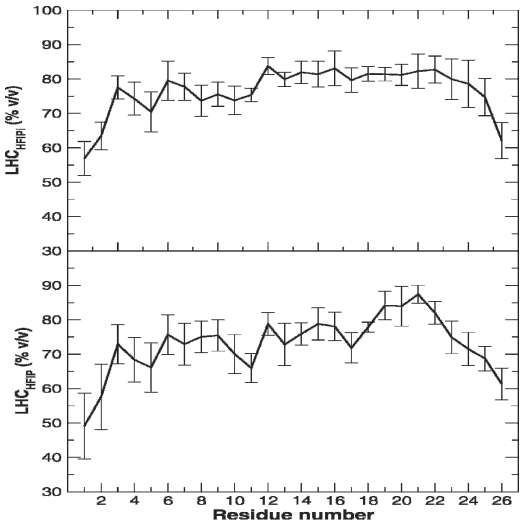

Figure 7. Average local HFIP concentration within a distance of 0.6 nm from the C_α atom of each residue of melittin, calculated using the full trajectory of both simulations. Bars indicate the standard deviations.

simulations are in agreement with the model of HFIP aggregation. In the case of the HFIPi simulation, it is possible to distinguish an inhomogeneous coating of the HFIP around the peptide. The presence of microheterogeneity of the HFIP/water mixture has been evidenced by light scattering data (Kuprin et al. 1995; Hong et al. 1999; Gast et al. 2001) and theoretical MD calculations (Fioroni et al. 2001). The clustering effect was also proposed by Gerig (2004) to give an interpretation of the NMR cross-relaxation rate measurements. Using a simplified model that accounts for the aggregation of the HFIP molecules in water, it results in a local concentration of HFIP around the peptide of 1.6 times the bulk concentration. Our results show that the average local concentration ($\approx$76% [v/v]) can be compared with this estimation, providing further microscopic evidence to the stabilization mechanism of fluorinated solvents.

The present simulations indicate that accumulation of HFIP around melittin is site-specific. The HFIP concentration around α-helical peptide regions is higher than in regions of irregular peptide backbone (near the kink or the ends of the peptide). Similar to TFE (Roccatano et al. 2002), HFIP molecules aggregate around the solute preventing the formation of hydrogen bonds with water molecules that can disrupt the α-helix structure (Pande et al. 1998; Walgers et al. 1998). The interactions between the peptide and HFIP do not displace the peptide–peptide interactions that stabilize the secondary structure. In the case of HFIP, the large molecular size can further deplete the possible interactions of HFIP with the backbone melittin atoms, enhancing the α-helix stabilization.

The origins of the stabilization mechanism may thus be both entropic and enthalpic. We noticed that the hydrophobic cosolvent tends to cluster around peptide regions rich in hydrophobic side chains. This effect tends to displace ordered water molecules from the vicinities of both HIFP and hydrophobic side chains, with a clear entropic gain for the final configuration of the system. Moreover, once water is excluded from the immediate vicinity of the peptide, intramolecular hydrogen bonds can form and stabilize, yielding a net favorable energetic contribution. Although, as stated above, the simulations are still too short to determine these effects quantitatively, the qualitative picture points to a combination of factors favoring peptide coating by HIFP.

It is also interesting to note the very good correspondence (residues 9–11; $\alpha = 77^\circ$) of the angular kink observed in the simulation with the NMR-determined structures (Gerig 2004). Furthermore, the formation of α-helix hairpin structure with a similar angular kink was observed in a theoretical study of melittin in the presence of POPC lipid bilayer (Lin and Baumgaertner 2000), but in the DPPC and DMPC lipid bilayer, a more extended structure was observed (Bernèche et al. 1998; Bachar and Becker 2000). In the last two cases, the simulation length was, however, limited to 500 psec. Our MD study indicates that the angle between helical segments is not static but can adopt a wide range of values. This might be of functional importance for the mechanism of membrane binding and insertion. Finally, the present comparative MD simulations also indicate a secondary-structure-stabilizing effect induced by the presence of counter-ions. In water the presence of counter-ions slows down the decay of secondary structure of melittin. Although this effect may be a purely kinetic effect (longer simulation may lead to a similar decay effect as seen in water), it is in

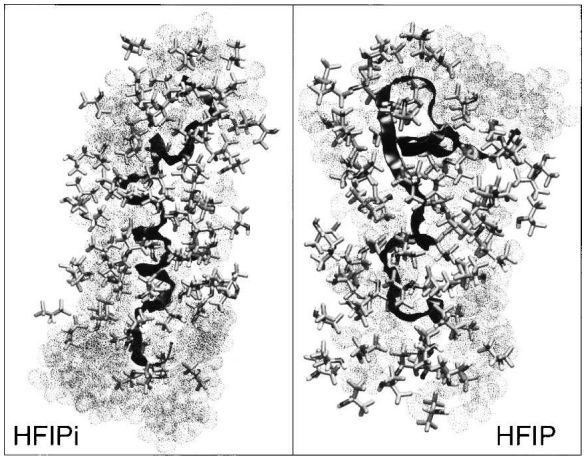

Figure 8. Snapshots of the last frame of the HFIPi and HFIP simulations. The peptide is represented as ribbon, and the solvent molecules within 0.6 nm are shown. The peptide is oriented with the C-ter at the *bottom*. Water molecules are represented as dotted surfaces.

qualitative agreement with experimental data. In fact, high salt concentrations and low pH increase the presence of α-helices in the tetrameric melittin form (Brown et al. 1980; Iwadate et al. 1998). In case of the HFIP mixture simulations, salt concentration still plays an important role. In fact, in the case of HFIP simulation, although to a lesser extent, the secondary structure is lost in the course of the simulation. However, the presence of HFIP retards the loss of secondary structure, extending the lifetime of the α-helix over a longer timescale than in pure water simulation (SPC).

Conclusions

In this study, we have used molecular dynamics simulations to analyze the effect of HFIP on the stability of the melittin peptide. The structural data evidence a very good correspondence with the experimental NMR data. The inclusion of counter-ions partly enhances the stability of the helical peptide structure, in agreement with experimental observations. Furthermore, the simulations show that in a HFIP/water mixture the organic cosolvent aggregates around the peptide, forming a matrix that partly excludes water. The nonuniform distribution of the HFIP around the peptide, supports the hypothesis of the presence of HFIP clusters that interact with the peptide. This, in turn, promotes the formation of local interactions and, as a consequence, ordered secondary structure. By displacing water from the surface, HFIP has several effects: First, it removes alternative hydrogen-bonding partners and, second, it provides a low dielectric environment. Together, these factors favor the formation of intrapeptide hydrogen bonds. The results are in line with previous simulation studies with TFE/water mixture, indicating a similar coating effect that promotes secondary structure stabilization.

Materials and methods

The starting conformation for the simulations of the melittin peptide was taken from the 0.2-nm-resolution crystal structure (PDB entry 2MLT) (Anderson et al. 1980). The peptide was protonated according to the experimental conditions (pH 2). The C-terminal residue was aminated. The peptide was centered in a cubic box and solvated with SPC water (Berendsen et al. 1987) or with a mixture of SPC water and HFIP molecules. We have used 3000 water molecules for the pure water simulations, and 4000 water and 350 HFIP molecules for the 35% (v/v) HFIP mixture. All solvent molecules with any atom within 0.15 nm of the peptide were removed. The concentration of the HFIP/SPC water mixture corresponds approximately to 35% v/v.

For the simulations with counter-ions (abbreviated SPCi and HFIPi for the water and HFIP/water mixture, respectively), six Cl^- counter-ions were added to neutralize the total charge of the systems. This was achieved by replacing water molecules at the most positive potential. The abbreviations SPC and HFIP will be used to indicate the simulations in water and HFIP/water mixture, respectively. The GROMOS96 force field (van Gunsteren et al. 1996) was used to describe the peptide. For the HFIP, the model proposed by Fioroni et al. (2001) was used. This model was optimized to reproduce the physicochemical properties of the pure liquid and mixtures with water. The model has been found in good agreement with the experimental data based on X-ray, neutron scattering, and NMR of the pure liquid as well as the mixtures (Yoshida et al. 2003).

All the systems were initially energy-minimized with the steep est descent method for 1000 steps. During the MD simulations, the peptide and the rest of the system were coupled separately to the temperature bath. The temperature was maintained close to the intended values (300 K) by weak coupling to an external temperature bath using a coupling time $\tau_T = 0.1$ psec (Berendsen et al. 1984). The pressure was kept constant at $P_0 = 1$ by weak coupling to a bath of constant pressure with a coupling time $\tau_P = 0.5$ psec (Berendsen et al. 1984). The LINCS algorithm (Hess et al. 1997) was used to constrain all bond lengths. For the water molecules, the SETTLE algorithm (Miyamoto and Kollman 1992) was used. A relative dielectric permittivity, $\varepsilon_r = 1$, and a time step of 2 fsec were used. A twin-range cutoff was used for the calculation of the nonbonded interactions. The short-range cutoff radius was set to 0.8 nm and the long-range cutoff radius, to 1.4 nm, for both Coulombic and Lennard-Jones interactions. No reaction field corrections beyond the long-range cutoff were included in the cutoff simulations. Interactions within the short-range cutoff were updated every time step, whereas interactions within the long-range cutoff were updated every five time steps together with the pair-list.

All atoms were given an initial velocity obtained from a Maxwellian distribution at the desired initial temperature. All the simulations were equilibrated by 50 psec of MD runs with positional restraints on the peptide to allow the relaxation of the solvent molecules. These first equilibration runs were followed by another 50-psec run without position restraints on the peptide. The production runs, after equilibration, were 100 nsec long.

Analysis of the simulations

The secondary structure of the peptides was analyzed using the DSSP criteria (Kabsch and Sander 1983). The α-helicity was calculated using the criterion of Hirst and Brooks (1995). Cluster analysis was performed using the Jarvis-Patrick method (Jarvis and Patrick 1973): A structure is added to a cluster when this structure and a structure in the cluster have each other as neighbors and they have at least P neighbors in common. The neighbors of a structure are the M closest structures or all the structures within a cutoff, based on the root mean square deviation between backbone atoms. In our case, P was 3, M was 10, and the RMSD was 0.1 nm.

The angle between helical axes was calculated using the MOLMOL program (Koradi et al. 1996). For each simulation frame, the boundary residues of the two helices are evaluated and used to perform the calculation of the helical axes. The interproton distances were calculated from the simulations as $\langle r^{-6}\rangle^{-1/6}$ averages (Tropp 1980).

The concentration (% v/v) of HFIP molecules around the peptide residues, named local HFIP concentration (LHC), was evaluated from the cumulative number of water $[n_w(r)]$ and HFIP $[n_H(r)]$ molecules present within a distance r from the C_αs of the single residues using the following relation:

$$LHC(r) = \frac{V_m^H n_H(r)}{\left[V_m^H n_H(r) + V_m^w n_w(r)\right]} 100 \qquad (1)$$

where $V_m^H = 0.1$ and $V_m^w = 0.019$ L/mol are the average excluded volumes for HFIP and water molecules, respectively (Marcus 1998). All the MD runs and the analysis of the trajectories were performed using the GROMACS software package (Berendsen et al. 1995; Lindahl et al. 2001).

References

Anderson, D., Terwilliger, T.C., Wickner, W., and Eisenberg, D. 1980. Melittin forms crystals which are suitable for high resolution X-ray structural analysis and which reveal a molecular 2-fold axis of symmetry. *J. Biol. Chem.* **255:** 2578–2582.

Bachar, M. and Becker, O.M. 2000. Protein-induced membrane disorder: A molecular dynamics study of melittin in a dipalmitoylphosphatidylcholine bilayer. *Biophys. J.* **78:** 1359–1375.

Berendsen, H.J.C., Postma, J.P.M., van Gunsteren, W.F., Di Nola, A., and Haak, J.R. 1984. Molecular dynamics with coupling to an external bath. *J. Chem. Phys.* **81:** 3684–3690.

Berendsen, H.J.C., Grigera, J.R., and Straatsma, T.P. 1987. The missing term in effective pair potentials. *J. Phys. Chem.* **91:** 6269–6271.

Berendsen, H.J.C., van der Spoel, D., and van Drunen, R. 1995. GROMACS: A message-passing parallel molecular dynamics implementation. *Comp. Phys. Comm.* **91:** 43–56.

Bernèche, S., Nina, M., and Roux, B. 1998. Molecular dynamics simulation of melittin in a dimyristoylphosphatidylcholine bilayer membrane. *Biophys. J.* **75:** 1603–1618.

Brown, L.R., Lauterwein, J., and Wüthrich, K. 1980. High-resolution ^{1}H-NMR studies of self-aggregation of melittin in aqueous solution. *Biochim. Biophys. Acta* **622:** 231–244.

Buck, M. 1998. Trifluoroethanol and colleagues: Cosolvents come of age. Recent studies with peptides and proteins. *Quart. Rev. Biophys.* **31:** 297–355.

Colombo, G., Roccatano, D., and Mark A.E. 2002. Folding and stability of the three-stranded β-sheet peptide βnova: Insights from molecular dynamics simulations. *Proteins* **46:** 380–392.

Colombo, G., De Mori, G.M.S., and Roccatano, D. 2003. Interplay between hydrophobic cluster and loop propensity in β-hairpin formation: A mechanistic study. *Protein Sci.* **12:** 538–550.

Diaz, M.D., Fioroni, M., Burger, K., and Berger, S. 2002. Evidence of complete hydrophobic coating of bombesin by trifluoroethanol in acqueous solution: An NMR spectroscopic and molecular dynamics study. *Chem. Eur.* **8:** 1663–1669.

Fioroni, M., Burger, K., Mark, A.E., and Roccatano, D. 2001. A model of 1,1,1,3,3,3-hexafluoropropan-2-ol for molecular dynamics simulations. *J. Phys. Chem. B* **105:** 10967–10975.

Fioroni, M., Diaz, M.D., Burger, K., and Berger, S. 2002. Solvation phenomena of a tetrapeptide in water/trifluoroethanol and water/ethanol mixtures: A diffusion NMR, interolecular NOE and molecular dynamics study. *J. Am. Chem. Soc.* **124:** 7737–7744.

Gast, K., Siemer, A., Zirwer, D., and Damaschun, G. 2001. Fluoroalcohol-induced structural changes in proteins: Some aspects of cosolvent–protein interactions. *Eur. Biophys. J.* **30:** 273–283.

Gerig, J.T. 2004. Structure and solvation of melittin in 1,1,1,3,3,3-hexafluoro-2-propanol/water. *Biophys. J.* **86:** 3166–3175.

Hess, B., Bekker, H., Berendsen, H.J.C., and Fraaije, J.G.E.M. 1997. LINCS: A linear constraint solver for molecular simulations. *J. Comp. Chem.* **18:** 1463–1472.

Hirota, N., Mizuno, K., and Goto, Y. 1997. Cooperative α-helix formation of β-lactoglobulin and melittin induced by hexafluoroisopropanol. *Protein Sci.* **6:** 416–421.

Hirst, J.D. and Brooks, C.L. 1995. Molecular dynamics simulations of isolated helices of myoglobin. *Biochemistry* **34:** 7614–7621.

Hong, D.-P., Hoshino, M., Kuboi, R., and Goto, Y. 1999. Clustering of fluorine-substituted alcohols as a factor responsible for their marked effects on proteins and peptides. *J. Am. Chem. Soc.* **121:** 8427–8433.

Ibragimova, G.T. and Wade, R.C. 1998. Importance of explicit salt ions for protein stability in molecular dynamics simulation. *Biophys. J.* **74:** 2906–2911.

Iwadate, M., Asakura, T., and Williamson, M.P. 1998. The structure of the melittin tetramer at different temperatures. An NOE-based calculation with chemical shift refinement. *Eur. J. Biochem.* **257:** 479–487.

Jarvis, R.A. and Patrick, E.A. 1973. Clustering using a similarity measure based on shared near neighbors. *IEEE Trans Comp.* **22:** 1025–1034.

Jasanoff, A. and Fersht, A. 1994. Qualitative determination of helical propensities from trifluoroethanol titration curves. *Biochemistry* **33:** 2129–2135.

Kabsch, W. and Sander, C. 1983. Dictionary of protein secondary structure: Pattern recognition of hydrogen-bonded and geometrical features. *Biopolymers* **22:** 2576–2637.

Kempe, M.D., Buckley, P., Yuan, P., and Prendergast, F.G. 1997. Main chain and side chain dynamics of peptides in liquid solution from ^{13}C NMR: Melittin as a model peptide. *Biochemistry* **36:** 1678–1688.

Koradi, R., Billiter, M., and Wültrich, K. 1996. MOLMOL: A program for display and analysis of molecular structures. *J. Mol. Graph.* **14:** 51–55.

Kuprin, S., Grauslund, A., Ehrenberg, A., Koch, M.H.J., and Horn, M.I. 1995. Nonideality of water–hexafluoropropanol mixtures as studied by X-ray small angle scattering. *J. Biochem. Biophys. Res. Comm.* **217:** 1151–1156.

Lin, J.H. and Baumgaertner, A. 2000. Molecular dynamics simulations of hydrophobic and amphiphatic proteins interacting with a lipid bilayer membrane. *Comp. Theor. Polymer Sci.* **10:** 97–102.

Lindahl, E., Hess, B., and van der Spoel, D. 2001. GROMACS 3.0: A package for molecular simulation and trajectory analysis. *J. Mol. Mod.* **7:** 306–317.

Liu, H.L. and Hsu, C.-M. 2003. The effect of solvent and temperature on the structural integrity of monomeric melittin by molecular dynamics simulations. *Chem. Phys. Lett.* **375:** 119–125.

Marcus, Y. 1998. *The properties of solvents*. Wiley Series in Solution Chemistry, Vol. 4. John Wiley, Chichester-New York.

Miyamoto, S. and Kollman, P.A. 1992. SETTLE: An analytical version of the SHAKE and RATTLE algorithms for rigid water models. *J. Comp. Chem.* **13:** 952–962.

Pande, V.S., Grosberg, A.Y., Tanake, T., and Rokhsar, D.S. 1998. Pathways for protein folding: Is a new view needed? *Curr. Opin. Struct. Biol.* **8:** 68–79.

Pfeiffer, S., Fushman, D., and Cowburn, D. 1999. Impact of Cl^- and Na^+ ions on simulated structure and dynamics of βark1 ph domain. *Proteins* **35:** 206–217.

Roccatano, D., Colombo, G., Fioroni, M., and Mark, A.E. 2002. Mechanism by which 2,2,2-trifluoroethanol/water mixtures stabilize secondary-structure formation in peptides: A molecular dynamics study. *Proc. Natl. Acad. Sci.* **99:** 12179–12184.

Sessions, R.B., Gibbs, N., and Dempsey, C.E. 1998. Hydrogen bonding in helical polypeptides from molecular dynamics simulations and amide hydrogen exchange analysis: Alamethicin and melittin in methanol. *Biophys. J.* **74:** 138–152.

Tropp, J. 1980. Dipolar relaxation and nuclear Overhauser effects in nonrigid molecules: The effect of fluctuating internuclear distances. *J. Chem. Phys.* **72:** 6035–6043.

van Gunsteren, W.F., Billeter, S.R., Eising, A.A., Hünenberger, P.H., Krüger, P., Mark, A.E., Scott, W.R.P., and Tironi, I.G. 1996. *Biomolecular simulation: The GROMOS96 manual and user guide*. Hochschulverlag AG an der ETH Zürich, Zürich.

Walgers, R., Lee, T.C., and Cammers-Goodwin, A. 1998. An indirect chaotropic mechanism for the stabilization of helix conformation of peptides in aqueous trifluoroethanol and hexafluoro-2-propanol. *J. Am. Chem. Soc.* **120:** 5073–5079.

Walser, R., Hünenberger, P.H., and van Gunsteren, W.F. 2001. Comparison of different schemes to treat long-range electrostatic interactions in molecular dynamics simulations of a protein crystal. *Proteins* **44:** 509–519.

Yoshida, K., Yamaguchi, T., Adachi, T., Otomo, T., Matsuo, D., Takamuku, T., and Nishi, N. 2003. Structure and dynamics of hexafluoroisopropanol–water mixtures by X-ray diffraction, small-angle neutron scattering, NMR spectroscopy, and mass spectrometry. *J. Chem. Phys.* **119:** 6132–6142.